Modelling Sub-Neptunes with MESA

Catherine Slaughter

March 24, 2023

1 Introduction

Gas giants are a class of planet that are believed to be disproportionately over-represented in the set of observed exoplanets to date. They are of interest to us because of what they have revealed (and, in some ways, disproven) about solar system formation, and the origins of our own home. However, despite having a wealth of new gas giant exoplanet observations in recent years (not to mention the four in our own backyard) we know remarkably little about the interior structure and evolutions of these planets.

While originally developed to model stellar structure and evolution, we can make use of the Modules for Experiments in Stellar Astrophysics (MESA, Paxton et al. (2011, 2013, 2015, 2018, 2019); Jermyn et al. (2023)) software to study sub-Neptune gas giants. In doing so, we exploit the similarities in the equations governing the interior structure (such as hydrostatic equilibrium, energy transport, etc.) between stars and such planets.

2 Methods

In order to model a set of isolated sub-Neptune exoplanets, running the MESA code is broken down into five general steps.

Step One: Create the Planet

We begin by creating a core-less planet composed of Hydrogen and Helium. The initial mass of this planet is set to $30M_{\oplus}$, and the radius to 3 Jupiter-radii. These values are arbitrarily large. Planets have a large radius when they are initially forming, and MESA will be able to bring the planet to its true size in the next steps.

Step Two: Add Planetary Cores

In order to create a core to a given model, MESA needs a core mass and density. For the purposes of this project, the core composition is assumed to be similar to the overall composition of Earth. Meaning that, for a given core mass, the core radius can be determined via the relation (Valencia et al., 2007):

$$\frac{R_{core}}{R_{\oplus}} = \left(\frac{M_{core}}{M_{\oplus}}\right)^{0.27} \tag{1}$$

In this context, the mass of the core is a user-chosen input, so we solve for R and calculate the average core density.

$$\rho_{\text{core}} = \frac{M_{\text{core}}}{(4/3)\pi R_{\text{core}}^3} \tag{2}$$

This process is done for five different values of M_{core}: $3M_{\oplus}$, $5M_{\oplus}$, $7M_{\oplus}$, $10M_{\oplus}$, $12M_{\oplus}$, and the resulting planetary models with cores are created in MESA.

Step Three: Reduce the Planets' Masses

Besides the planetary core mass, the other parameter we are interested in probing is the mass fraction of the envelope, f_{env}, for each planet. The mass fraction can be calculated as follows:

$$f_{env} = \frac{M_{env}}{M_p} \tag{3}$$

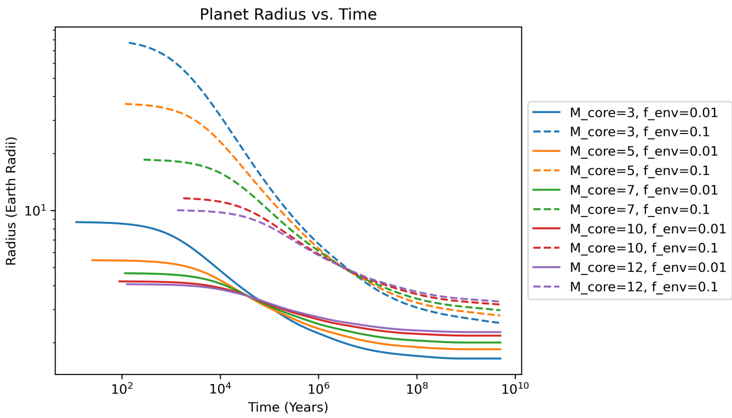

Figure 1: Planetary radii vs. time for the 10 models studied. Colour indicates core mass, while line style reflects envelope mass fraction. Models with greater mass fraction (0.1) is represented by the dotted lines, and those with lesser mass fraction (0.01) by the solid lines. Note that all the planets start at slightly different times as a result of setting the initial entropy at the base of the envelope.

Where M_{env} is the mass of the envelope and $M_p = M_{core} + M_{env}$ is the total mass of the planet. Because MESA takes in the total planet mass for simulations, we need to solve this equation for M_p as a function of f_{env} and M_{core}.

$$M_p = \frac{M_{core}}{1 - f_{env}} \tag{4}$$

We are interested in studying two values of f_{env}, 0.1 and 0.01, for each core mass, so we are left with 10 different planetary models to simulate.

Step Four: Set Initial Entropy

The final preparation in order to actually evolve these planetary models involves setting the initial entropy at the base of each planet's envelope. For these purposes, the initial entropy is set to $9kB/baryon$ at the simulation start time. In order to ensure this value, an artificial central luminosity ($2 \times 10^{27} erg/s$) is set, and the planet models created in Step 3 are evolved very slightly until the initial entropy limit is hit.

Step Five: Evolve the Planets

In order to fully run the simulation, the artificial internal luminosity must be brought to a more realistic value. we multiply the core mass of each model (converted to grams) with a standard core regeneration rate to obtain this value.

$$5 \times 10^8 (erg/g/s) * M_{core}(g) \tag{5}$$

From here, each of the 10 planetary models is finally run for 5Gyr of simulation time via MESA.

3 Results

After the simulations were finished running on MESA, the resulting profile and history data files were read in (using the PyMesaReader toolkit[1]), and several plots made.

Planet Radius vs. Evolutionary Time

Figure 1 shows the evolution of the planetary radii with time. It should be noted that the planets appear to all start at different times. This is a result of Step 4 as outlined in section 2.

In this plot, it can be seen that the planets with larger envelope mass fractions tend to have larger radii. This makes sense, as these planets are larger overall but do not have the high densities required for radii to become smaller with increased mass, as is sometimes seen in stars. However, we can also see that these stars generally lose more mass over time (as they have more mass that is lose-able), such that their final envelope mass fractions would be more on the order of $f_{env} = 0.01$.

[1] https://billwolf.space/py_mesa_reader/

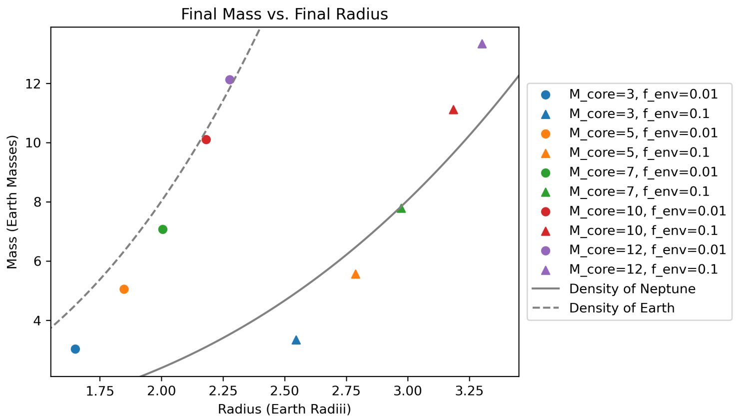

Figure 2: The final masses and radii for the 10 models. Again, colour indicates core mass while marker shape indicates mass envelope fraction (triangles for the larger, circles for the smaller). Additionally, the two grey lines represent the densities of Earth (dashed line) and Neptune (solid)

On the flip side, for a given f_{env}, the planets with smaller core masses tend to start out larger and shrink more substantially. This is because the gravitational pull from their core is not strong enough to counterbalance internal gas forces, causing the envelope to expand out and, ultimately, be lost to space. That being said, all the models shown do lose some of their envelope, as seen in the general reduction in radius across the board.

Final Mass vs. Final Radius

Figure 2 shows a plot of the masses and radii of the 10 models at the final simulation time step, as well as lines corresponding to the densities of Earth and Neptune, for reference.

As was true in Figure 1, this plot shows that the planets with smaller envelope mass fractions, in general, have smaller radii. We can see that the densities of the planets with smaller f_{env} are more like that of Earth, while the densities of those with larger f_{env} are closer to Neptune. This makes sense, given that the smaller f_{env} planets densities are more well dominated by the core, which is defined to be similar in composition to Earth. That being said, neither set of planets lies perfectly along a line of constant density, where the smaller-mass planets are generally less dense. This, again, is likely a reflection of the core's ability to "hold on" to the envelope.

Radiative and Adiabatic Gradients vs. Radius

Figure 3 Shows the Radiative and Adiabatic Gradients for each of the 10 models created vs their radii. Although each model has its own subplot, the axes over the plots are standardised for comparison purposes.

Again, we see that the planets with the lower envelope mass fraction have a smaller radius in general. For all the models, we see the adiabatic gradient stays relatively constant for most of the envelope, wile the radiative gradient varies more. In particular, we see two large spikes in the radiative gradient just before plummeting near the envelope's outer surface. For the stars with larger envelopes, there is somewhat more variation in the radiative gradient before this spike, with most showing a distinct dip.

The radiative gradient is also larger than the adiabatic throughout most of the envelope, until very near the surface. Using the simple Schwarzchild Criterion, we know energy transport is dominated by radiation when:

$$\nabla_{rad} < \nabla_{ad} \tag{6}$$

This makes sense with our plots, as we would expect energy to be transported by radiation near the surface. This, in turn, indicates that for all the models, the majority of envelope's energy transport is via convection.

Temperature-Pressure Profile

Figure 4 shows the Temperature-Pressure profiles for all 10 models, in both log-log space and normal linear space. While this plot is typically represented in log-log space in most literature, both are shown here to better illustrate how the models diverge nearer the bottom of the envelope.

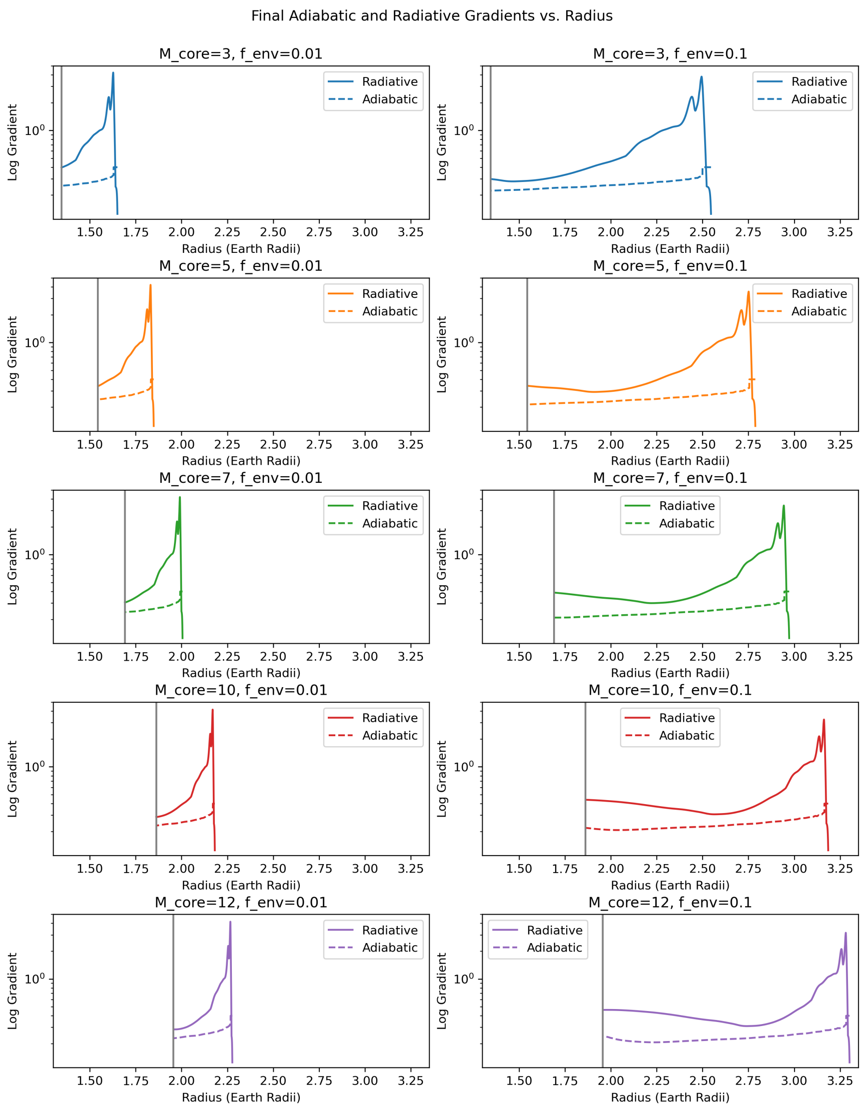

Figure 3: The radiative (solid) and adiabatic (dashed) gradients in the envelope vs radius for all 10 models. Model parameters are expressed in subplot titles. Each subplot coloured according to mass in order to correspond with the other figures in this report. The grey vertical line indicates the core radius, as calculated by Equation 1.

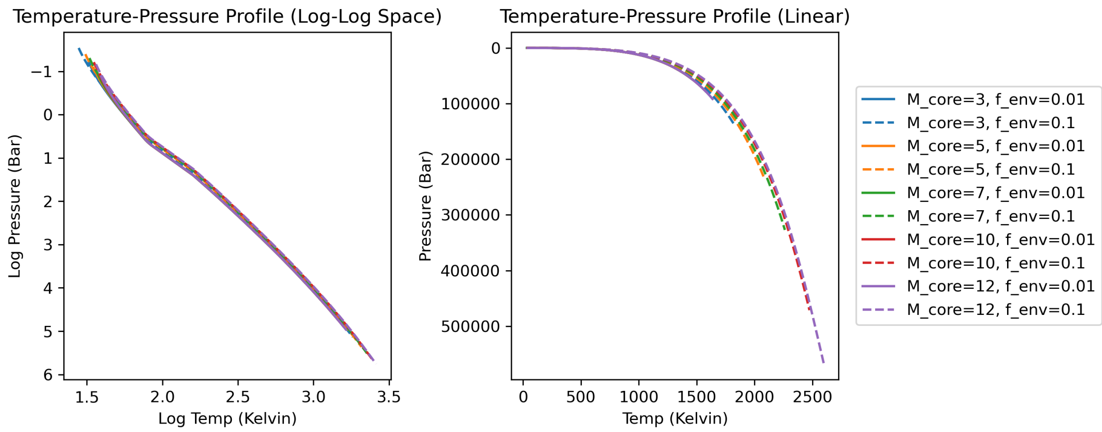

Figure 4: The Temperature-Pressure profiles for all models, in log-log (left) and linear (right) space. Again, color represents core mass while line style represents envelope mass fraction.

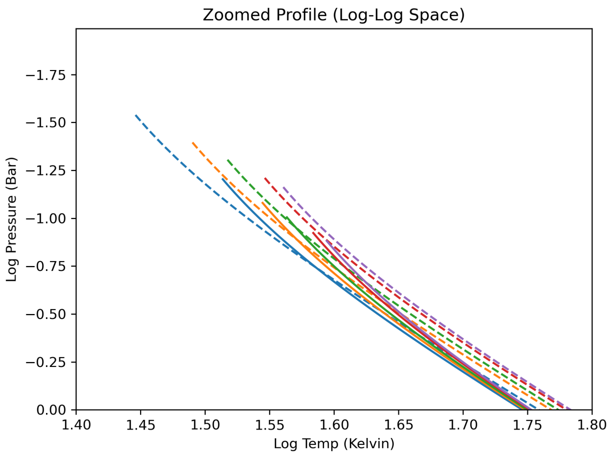

Figure 5: The same plot as in the left frame of Figure 4, but zoomed in to show detail.

It can be seen from the log-log plot that while the profiles are largely very similar, there is some separation near the outer surface of the envelope. Zooming in on this region (Figure 5), we can see that, for a given envelope mass fraction, the planets with lower core masses generally have lower pressures and lower temperatures at their very edges.

Additionally, the linear plot shows a separation in the different models nearer the bottom of the envelope. It is worth noting that the models with smaller f_{env} generally do not reach the high temperatures and pressures as those with large f_{env}.

When comparing this plot to Fig.2 of Guillot et al. (2022), it appears that, these planets are likely entirely made up of molecular hydrogen. According to that plot, metallic hydrogen begins when $log(pressure) >\sim 6.2$, so our planets (topping out at just below 6) would need to be somewhat more massive to have metallic hydrogen. Similarly, these planet models are not hot enough to reach the continuous phase transition into atomic hydrogen.

4 Discussion

While the results of this practicum are self-consistent and fairly reasonable, there are several large assumptions being made in the creation of these models which limit how applicable they may be to observed sub-Neptune exoplanets.

One such assumption is that of the planets' core compositions (Equation 1), as we saw in Figure 1, the initial state of the planet core is very important to the time-evolution of the planet's radius via envelope loss. Changing this composition would very easily impact this. Relatedly, we also assume that there is a clear cutoff between the core and the envelope, which recent studies into solar system gas giant planets (Miguel et al., 2022) indicate may not be as reasonable as once thought.

We also assume that the planetary envelopes are composed primarily of hydrogen and helium. This again has implications for envelope loss, based on the overall density of the gas in the envelope. Additionally, our conclusions about energy transport from Figure 3 are likely incomplete. We make use of the Schwarzchild Criterion to determine where we expect convection or radiation to dominate, when in reality, a more complete picture would use the Ledoux Criterion, which also accounts for the heavy element gradient in the envelope. The planetary composition also impacts our conclusions from Figure 4, as increased heavy elements may effect gas pressure.

5 Conclusion

Often times in astronomy, we find clever ways to make use of existing tools to study new systems or phenomena. The use of MESA, a stellar structure and evolution code, to study gas giant sub-Neptune planet structure is one great example of this. In this practicum, we created models of 10 such planets with different internal planetary structures, and simulated them over 5Gyr using MESA. In doing so, we found how a planet's core mass and initial envelope mass fraction can impact its structure and long-term evolution. This is reflected in planetary radii, total masses and densities, energy transport, and internal states of matter.

References

Guillot, T., Fletcher, L. N., Helled, R., et al. 2022, arXiv e-prints, arXiv:2205.04100, doi: 10.48550/arXiv.2205.04100

Jermyn, A. S., Bauer, E. B., Schwab, J., et al. 2023, ApJS, 265, 15, doi: 10.3847/1538-4365/acae8d

Miguel, Y., Bazot, M., Guillot, T., et al. 2022, A&A, 662, A18, doi: 10.1051/0004-6361/202243207

Paxton, B., Bildsten, L., Dotter, A., et al. 2011, ApJS, 192, 3, doi: 10.1088/0067-0049/192/1/3

Paxton, B., Cantiello, M., Arras, P., et al. 2013, ApJS, 208, 4, doi: 10.1088/0067-0049/208/1/4

Paxton, B., Marchant, P., Schwab, J., et al. 2015, ApJS, 220, 15, doi: 10.1088/0067-0049/220/1/15

Paxton, B., Schwab, J., Bauer, E. B., et al. 2018, ApJS, 234, 34, doi: 10.3847/1538-4365/aaa5a8

Paxton, B., Smolec, R., Schwab, J., et al. 2019, ApJS, 243, 10, doi: 10.3847/1538-4365/ab2241

Valencia, D., Sasselov, D. D., & O'Connell, R. J. 2007, ApJ, 656, 545, doi: 10.1086/509800